Reversible and Vapochromic Chemisorption of Ammonia by a Copper(II) Coordination Polymer

Wegeberg, Christina; Nielsen, David; Mossin, Susanne; Abrahams, Brendan F.; McKee, Vickie; McKenzie, Christine J.

Published in:
Australian Journal of Chemistry

Link to article, DOI:
10.1071/CH19264

Publication date:
2019

Document Version
Peer reviewed version

Reversible and Vapochromic Chemisorption of Ammonia by a Copper(II) Coordination Polymer

Christina Wegeberg,[a] David Nielsen,[b] Susanne Mossin,[b] Brendan F. Abrahams,[c] Vickie McKee,[a] Christine J. McKenzie[a]*

[a] Department of Physics, Chemistry and Pharmacy, University of Southern Denmark, Campusvej 55, 5230 Odense M, Denmark. E-mail: mckenzie@sdu.dk.

[b] Centre for Catalysis and Sustainable Chemistry, Department of Chemistry, Technical University of Denmark, Lyngby 2800, Denmark

[c] School of Chemistry, University of Melbourne. Parkville, Victoria, 3010, Australia

Keywords: ammonia · copper · coordination network · reversible sorption

Abstract

The single crystal X-ray structure determination of $\{[Cu(tpt)(o\text{-phthalate})]\cdot 3^1/_3(C_2H_2Cl_4)\}_n$ (tpt = 2,4,6-tri-4-pyridyl-1,3,5-triazine, $C_2H_2Cl_4$ = 1,1,2,2-tetrachloroethane = TCE) shows a 3D network in which Cu(II) centres are linked by 3-connecting tpt ligands with the topology of a 12,3 net. Cu(II) centres are further linked by *o*-phthalate dianions. The copper coordination geometry is square pyramidal, with *o*-phthalate oxygen donors *trans* to each other in the basal plane and the remaining positions taken by the pyridines of three linking tpt units. The solvent accessible void space is approximately 65%. The pale blue-green crystalline desolvate, obtained by heating to 200 °C or washing the TCE solvate with acetone is formulated as $[Cu(tpt)(o\text{-phthalate})]_n$. Powder X-ray diffraction and electron paramagnetic resonance spectroscopy show that the crystal structure and the Cu(II) geometry change upon desolvation. The crystalline desolvated phase sorbs two equivalents of ammonia per copper ion. The adduct, mauve $[Cu(tpt)(o\text{-phthalate})(NH_3)_2]_n$, shows reasonable crystallinity and is stable up to ca. 150 °C under ambient conditions before the reversible desorption (minimum 10 cycles) of the guest ammonia. The colour change and high desorption temperature, along with changes in *g*-values, is suggestive of chemisorption in two steps with Cu-amine bonding in the loaded phase.

Introduction

Coordination polymers (CPs) with high porosity[1] are a promising class of material for the storage,[2,3] sensing[4,5] and separation[6,7] of gases. Ammonia is targeted in this context since it is widely used in industry for production of plastics, fertilizers, refrigerators, explosives, nitric acid and intermediates for dyes and pharmaceuticals.[8] It is a colourless gas which is corrosive, toxic and chemically active. The detection of ammonia is important for human health, industry, agriculture, environment and protection from terrorism. However, achieving selective and reversible sorption of ammonia is a challenge due to its basicity. For example, Peterson *et al* have demonstrated using solid state MAS NMR studies that the uptake of ammonia by the CP $Cu_3(BTC)_2$ (BTC = 1,3,5-benzenetricarboxylate) (HKUST-1) is due to irreversible structural decomposition to $Cu(OH)_2$ and $(NH_4)_3BTC$.[9] In order to make the removal of ammonia efficient and useful for commercial application, CPs should show both thermal and chemical stability and be able to detect low levels of ammonia vapour.[10] Towards this goal Dincă and co-workers recently demonstrated that $Cu_3(HITP)_2$ (HITP = 2,3,6,7,10,11-hexaaminotriphenylene) can reversibly detect ammonia at concentrations as low as 0.5 ppm under dry inert N_2 atmosphere.[11] We have constructed a new copper containing CP based on 2,4,6-tri-4-pyridyl-1,3,5-triazine (tpt) and *o*-phthalate that can reversibly bind ammonia. The new material is stable to moisture and retains two equivalents of ammonia up to 150 °C under ambient atmosphere. We propose that these ammonia molecules are coordinated to the copper center and this occurs in a stepwise fashion.

Experimental Section

Materials

1,1,2,2-tetrachloroethane and K(Hphthalate) were purchased from Fluka. All other chemicals were purchased from Sigma Aldrich. Aqueous ammonia (28 - 30%) was used.

Instrumentation

IR spectra were recorded on a PerkinElmer Spectrum 65 (FT-ATR diamond anvil) on the neat samples. Thermal analysis was carried out on a Perkin Elmer TGA 4000 from 30-200 °C at 10 °C/min in a nitrogen atmosphere with a purge rate of 20 mL/min. PXRD measurements were performed on Rigaku Miniflex 600 X-Ray Diffractometer with Cu(Kα) (λ = 1.5409 Å, 40 kV, 15 mA) within the 2θ range 5 - 90°. Electron paramagnetic resonance (EPR) spectra were recorded using powdered samples on a Bruker EMX X-band spectrometer using the previously described setup.[12] The signal was quantified by double integration of

background-corrected spectra and compared to spectra obtained on four reference sample of solid solutions of $CuSO_4 \cdot 5H_2O$ in K_2SO_4. ^1H (400.12 MHz) and ^{13}C NMR (100.61 MHz) spectra were recorded on a Bruker Avance III 400 spectrometer, and the chemical shifts are denoted relative to the residual solvent peak ($CDCl_3$: δ_H 7.26 ppm; δ_C 77.16 ppm). Electrospray ionization (ESI) mass spectra were recorded in high-resolution positive ion-mode on a Bruker micrOTOF-Q II mass spectrometer.

Synthesis

2,4,6-tri-4-pyridyl-1,3,5-triazine (tpt)

Apart from the purification step, the synthesis was the same as that reported by Anderson *et al*[13]: KOH (126 mg, 2.25 mmol), 18-crown-6 (505 mg, 1.91 mmol) and 4-cyanopyridine (5.13 g, 49.3 mmol) were dissolved in decaline (10 ml) and stirred under N_2 flow for 3h at 200 °C. During this time the solution changes colour from orange to red to black. A brown solid precipitated on cooling the mixture to rt. This is isolated by filtration and subsequently suspended in warm water. The solids are then re-filtered and washed with acetone (1 x 5 ml) to give a fine grey powder.

Yield: 901 mg (18 %). ^1H NMR (400.12 MHz, $CDCl_3$): δ 8.94 (dd, *J* = 4.8, 1.6 Hz, 6H), 8.56 (dd, *J* = 4.4, 1.6 Hz, 6H) ppm. ^{13}C NMR (100.61, $CDCl_3$): δ 171.61, 151.19, 142.55, 122.43 ppm. ESI-MS (MeCN, pos. mod): found (calcd) *m/z* = 313.1119 (313.1196, $[tptH]^+$, $C_{18}H_{13}N_6$, 100 %), 335.1205 (335.1021, $[tptNa]^+$, $C_{18}H_{12}N_6Na$, 17 %)

$\{[Cu(tpt)(o\text{-phthalate})] \cdot 3^1/_3(C_2H_2Cl_4)\}_n$

Tpt (124.6 mg, 0.40 mmol) was dissolved in 1,1,2,2-tetrachloroethane (TCE, 40 ml) to give a colourless, clear solution after rapid stirring for a few hours. A solution of $Cu(NO_3)_2 \cdot 3H_2O$ (94.9 mg, 0.39mmol) and K(Hphthalate) (82.0 mg, 0.40 mmol) in MeOH (25 ml) was added, and the reaction mixture was stirred for one hour to obtain $[Cu(tpt)(o\text{-phthalate})] \cdot 3^1/_3(C_2H_2Cl_4)$ as a blue powder. This was isolated by vacuum filtration without washing. Yield: 413 mg (94 %) IR (KBr): *v* [cm^{-1}]: 3428 (m), 1617 (m), 1576 (m), 1519 (s), 1376 (s), 1315 (m), 1215 (w), 1160 (w), 1061 (m), 870 (w), 826 (w), 803 (m), 753 (w), 737 (w), 669 (w), 643 (m), 518 (w). PXRD shows a high degree of crystallinity.

Single crystals of $\{[Cu(tpt)(o\text{-phthalate})] \cdot 3^1/_3(C_2H_2Cl_4)\}_n$ could be grown by layering the TCE solution of tpt and the methanol solution of $Cu(NO_3)_2$ and K(Hphthalate) in a sealed vial. Turquoise seed crystals form at the interface of the two layers. These grow larger over several days. The single crystals used for SCXRD were mounted cryogenically, onto a glass fibre using oil for adherence, directly from the mother liquid by

using a stage mounted inside a dewar containing liquid N_2. Removal of the crystals from the solution phase to air under ambient conditions results in their visible macroscopic collapse to a powder within seconds.

[Cu(tpt)(*o*-phthalate)]$_n$

The powder form of {[Cu(tpt)(*o*-phthalate)]·$3^1/_3(C_2H_2Cl_4)$}$_n$ was suspended in acetone and then re-filtered to give a pale blue-green powder of [Cu(tpt)(*o*-phthalate)]$_n$. TGA does not show any mass loss up to 160° indicating that the TCE has been removed and not replaced by acetone. Yield: 97-100 %.

Gas-solid Reactions

[Cu(tpt)(*o*-phthalate)]$_n$ was exposed to the vapour evolved from aqueous ammonia in a sealed container. The solids change colour within minutes.

Crystallography

The data were collected at 150(2) K on a Bruker-Nonius ApexII CCD diffractometer using MoK_α radiation (λ = 0.71073 Å) and were corrected for Lorentz-polarisation effects and absorption (SADABS[14]). The structure was solved by dual space methods (SHELXT[15]) and refined on F^2 using all the reflections (SHELXL-2018[16]). All the non-hydrogen atoms of the framework were refined using anisotropic atomic displacement parameters and hydrogen atoms were inserted at calculated positions using a riding model. The aromatic ring of the phthalate group is disordered and was modelled with equal occupancy of two orientations. The large void space in the crystal contains diffuse electron density and this was treated using SQUEEZE[17]; a single large void of 2600 Å^3 (64.6 %) in the unit cell was estimated to contain 829 electrons corresponding to 10 molecules of $C_2H_2Cl_4$ per cell (820 electrons). Since the high angle data were very weak, the refinement was truncated at resolution 0.90 Å. Crystal data, data collection and structure refinement details are summarized in Table 1.

Table 1 Crystal data and structure refinement for {[Cu(tpt)(*o*-phthalate)]·$3^1/_3(C_2H_2Cl_4)$}$_n$.

Empirical formula	$C_{26}H_{16}CuN_6O_4 \cdot 3^1/_3(C_2H_2Cl_4)$
Formula weight	1099.44
Temperature/K	150.15
Crystal system	trigonal
Space group	$P3_1$
a/Å	16.0982(16)
b/Å	16.0982(16)
c/Å	17.9322(18)
Volume/Å^3	4024.6(9)

Z	3
ρ_{calc} g/cm^3	1.361
μ/mm^{-1}	1.108
F(000)	1645.0
Crystal size/mm^3	0.30 × 0.16 × 0.15
Radiation	Mo$K\alpha$ (λ = 0.71073)
Reflections collected	80783
Independent reflections	7141 [R_{int} = 0.1213, R_{sigma} = 0.0972]
Data/restraints/parameters	7141/777/389
Goodness-of-fit on F^2	1.017
Final R indexes [I>=2σ(I)]	R_1 = 0.0669, wR_2 = 0.1504
Final R indexes [all data]	R_1 = 0.1134, wR_2 = 0.1737
Largest diff. peak/hole / e Å^{-3}	0.89/-0.30
Flack parameter	0.09(3)

Results and Discussion

The structure of $\{[Cu(tpt)(o\text{-phthalate})]\cdot 3^1/_3(C_2H_2Cl_4)\}_n$

Single crystals of the turquoise CP $\{[Cu(tpt)(o\text{-phthalate})]\cdot 3^1/_3(C_2H_2Cl_4)\}_n$ were grown at the interface of the layers of TCE and MeOH over the course of a few days. The crystals were mounted on a glass fibre under cryogenic conditions as quickly as possible after removal from the mother liquor. The same material as a finely divided powder, can be prepared by mixing all reagents and stirring for one hr 1:1 TCE:MeOH. Both approaches give close to stoichiometric yields (> 94%). The powder X-Ray diffraction (PXRD) patterns for bulk macroscopically powdered samples of $\{[Cu(tpt)(o\text{-phthalate})].3^1/_3(C_2H_2Cl_4)_3\}_n$ shows that the material is a highly ordered crystalline structure with defined and sharp reflections at the lower angles (Figure S5).

The structure of $\{[Cu(tpt)(o\text{-phthalate})]\cdot 3^1/_3(C_2H_2Cl_4)\}_n$ was solved in the chiral (Sohncke) space group $P3_1$. The asymmetric unit comprises one copper ion, one tpt molecule and one (disordered) *o*-phthalate dianion (Figure 1), as well as some poorly defined solvate molecules. The copper ions are pentacoordinated and bonded to one pyridine from each of three tpt ligands, N1, N3 (under -x+y, -x+1, z+$^2/_3$), and N5 (under -y, x-y, z+$^1/_3$) as well as two carboxylate oxygen atoms from different *o*-phthalate units O1 and O4 (under -x+y, -x+1, z-$^1/_3$). The bond distances and approximate square pyramidal geometry at the copper ion are unremarkable (Table 2). The two oxygen donors are located *trans* to each other in the basal plane and N5 is the apical donor (Figure 1).

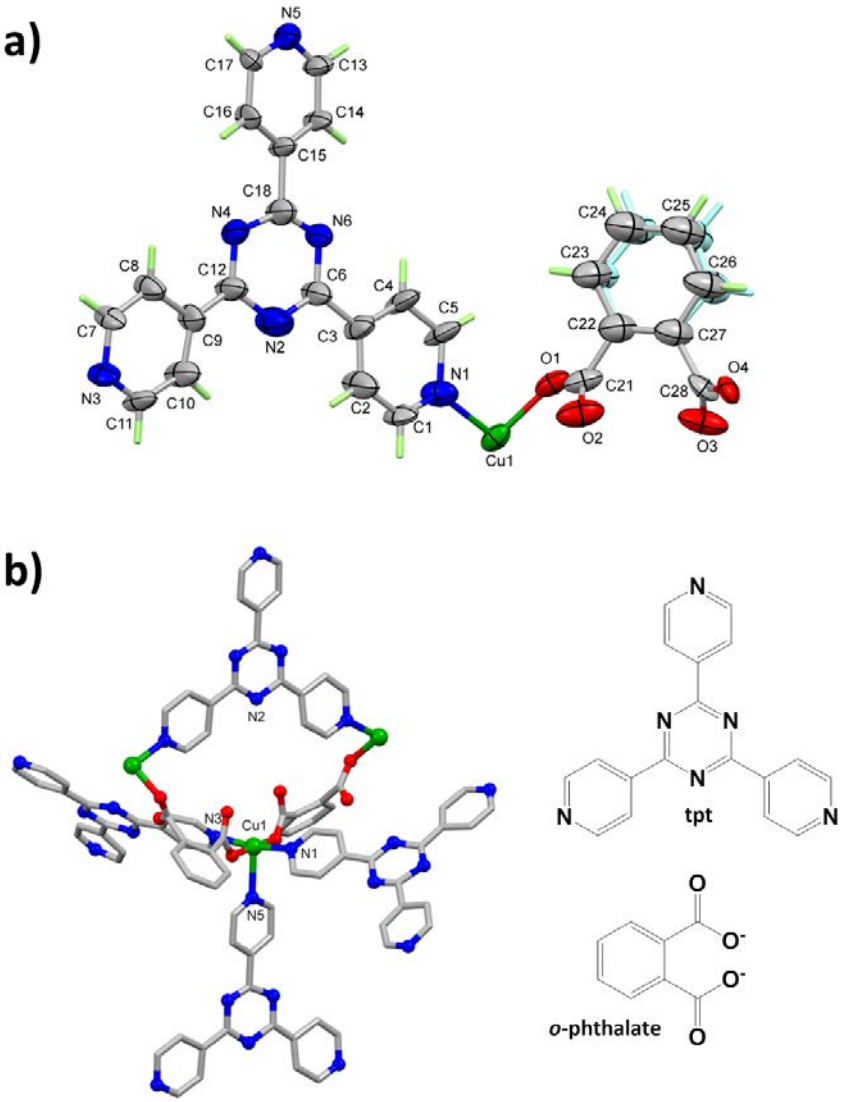

Figure 1*: The crystal structure of {[Cu(tpt)(o-phthalate)]solvate}$_n$ showing a) the asymmetric unit with 50% probability displacement ellipsoids; a second component of the phthalate disorder is shown in pale blue, hydrogen atoms are shown as sticks. b) the coordination environment of the copper ion (disorder removed for clarity).* Colour code: Cu green, O red, N blue and C grey.

Table 2. Selected geometric parameters (Å and °)

Cu1—O1	1.926 (8)	O1—Cu1—O4^{i}	177.7 (3)
Cu1—O4^{i}	1.953 (7)	O1—Cu1—N1	89.6 (3)
Cu1—N1	1.990 (9)	O4^{i}—Cu1—N1	90.1 (3)
Cu1—N3^{ii}	2.023 (9)	O1—Cu1—N3^{ii}	90.1 (3)
Cu1—N5^{iii}	2.370 (9)	O4^{i}—Cu1—N3^{ii}	90.6 (3)

		N1—Cu1—N3^{ii}	170.1 (4)
Cu1—O2	3.21 (1)	O1—Cu1—N5^{iii}	86.9 (3)
Cu1—O3^{i}	3.16 (7)	O4^{i}—Cu1—N5^{iii}	90.8 (3)
Cu1—N2^{iv}	6.92(1)	N1—Cu1—N5^{iii}	94.6 (4)
Cu1—Cu1^{iv}	7.8857(13)	N3^{ii}—Cu1—N5^{iii}	95.3 (4)

Symmetry codes: (i) -*x*+*y*, -*x*+1, *z*-$^{1}/_{3}$; (ii) -*x*+*y*, -*x*+1, *z*+$^{2}/_{3}$; (iii) -*y*, *x*-*y*, *z*+$^{1}/_{3}$, (iv) -y+1, 1+x-y, $^{1}/_{3}$+z

From a topological perspective the tpt ligand may be considered as a 3-connecting node with links to three Cu(II) centres. The Cu(II) centre on the other hand is a 5-connecting node forming links to three tpt ligands and two crystallographically equivalent Cu(II) ligands through bridging *o*-phthalate ligands. The resulting 3D network, composed of both 3- and 5-connecting nodes, is particularly complex and the topological description, based on consideration of these two nodes (point symbol: $(4.7^2)(4^3.6^2.7^4.8)$)[18] fails to easily convey the connectivity of the network. The 3D network may be more simply understood by ignoring, in the first instance, the bridging *o*-phthalate dianions and considering only the Cu-tpt network. Under these circumstances both the Cu centres and tpt ligand serve as 3-connecting nodes within a chiral network that belongs to the class of networks with an unusual "12,3" topology.

Throughout his career the structural chemist A. F. Wells categorised hundreds of inorganic compounds and was largely responsible for using mathematical nets to describe the connectivity of crystalline solids.[19,20] His approach involved identifying the connectivity of a node and then determining the shortest circuit in the structure involving the node. Whilst Wells was able to assign topological labels to inorganic structures he did, with remarkable insight, describe some mathematical nets such as a 12,3 net that did not have a recognised chemical counterpart at the time. The 12,3 net described by Wells is now represented by the 3-letter code twt.[21] A representation of the 12,3 net is presented in Figure 2(a) which shows parallel 6-fold double helices which are linked by connections normal to the direction of the helical axes. In this representation all nodes are identical but because the network cannot form with perfect trigonal nodes not all angles at the planar 3-connecting nodes are the same. The presence of parallel double helices results in the network being chiral. Within the family of uniform (n,3) nets considered by Wells, his 12,3 net occupies a position of special significance because of the phenomenon of self-entanglement as discussed later.

In the late 1980's and 1990's Robson employed a net-based based approach to design and describe coordination polymers and found that Wells' approach to representing connectivity to be particularly useful.[22,23] Workers such as O'Keeffe have also made important contributions in regards to the use of topological symbols to represent connectivity in chemical networks.[21,24] In regards to the 12,3 net described by Wells, Robson noted that the network can form in a strain-free manner if T-shaped and true

trigonal nodes are combined in a 1:1 ratio as indicated in Figure 2(b). In this case, with two distinct nodes, 3-fold double helices are formed instead of the 6-fold double helices.

In the structure of Ni(tpt)$(NO_3)_2$·solvate, described by Robson *et al.* in 1999,[25] tpt ligands serve as trigonal 3-connecting centres while the Ni(II) centres with *mer* configuration of pyridyl groups act as T-connecting centres. The remaining coordination sites of the 6-coordinate Ni(II) centre are occupied by disordered, non-bridging nitrate ions. Figure 2(b) thus provides a simplified schematic representation of the structure in which only the two types of 3-connecting centres are represented. To the best of our knowledge the $\{[Ni(tpt)(NO_3)_2]\cdot solvate\}_n$ was the first reported example of a chemical structure that has the 12,3 connectivity described by Wells. In 2013 Bu *et al.* reported a series of compounds which possessed the same Ni-tpt framework but with *o*-phthalate ligands in place of nitrate anions in $\{[Ni(tpt)(NO_3)_2]solvate\}_n$.[26] The *o*-phthalate ligands are bridging and provide additional links between the Ni(II) centres of the Ni-tpt network.

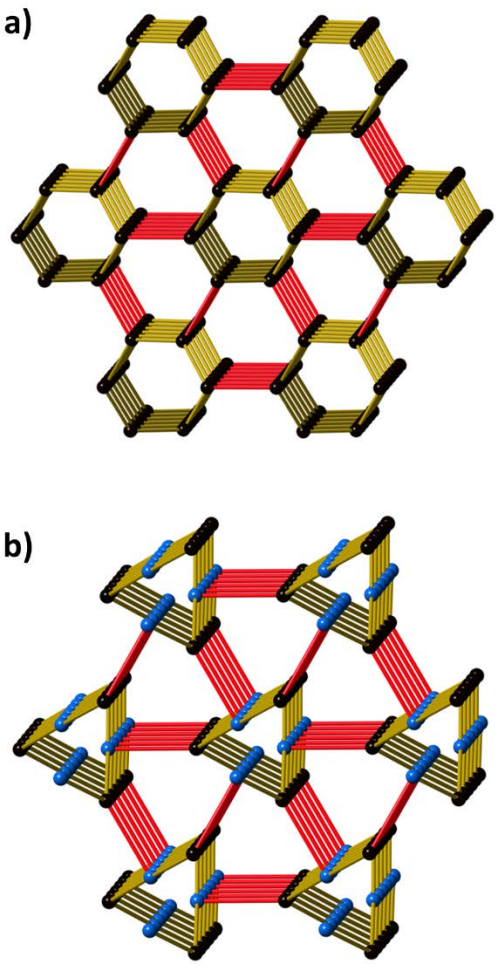

Figure 2. *Representations of 12,3 nets. a) Black spheres represent 3-connecting centres with all centres identical in an idealised network. b) Black spheres represent trigonal 3-connecting trigonal centres whilst blue spheres represent 3-connecting T-shaped centres. In each net, gold connections belong to double helices whilst red connections link the double helices and are orthogonal to the double helix axes.*

The Cu(II) network presented in this current work closely resembles Bu's compound, [Ni(tpt)(L)(H_2O)]·solvate (L= *o*-phthalate and substituted *o*-phthalate ligands) but with a square pyramidal Cu(II) centre in place of the octahderal Ni(II) centre whose sixth site is occupied by a water molecule. The adoption of the space group $P3_1$ by [Cu(tpt)(o-phthalate)]·solvate is in contrast to the higher symmetry space group, $P3_121$ (and its enantiomorphic partner, $P3_221$) found for {[Ni(tpt)(NO_3)$_2$]solvate}$_n$ and {[Ni(tpt)(L)]solvate}$_n$. Attempts to refine Cu(tpt)(o-phthalate)]·solvate in the $P3_121$ led to an unsatisfactory refinement of the *o*-phthalate anions. Despite the differences in space group symmetry, the structural similarity of the three compounds, {[Ni(tpt)(NO_3)$_2$]solvate}$_n$, {[Ni(tpt)(*o*-phthalate)(H_2O)]solvate}$_n$ and {[Cu(tpt)(*o*-phthalate)]solvate}$_n$ is clearly apparent with the metal-tpt 12,3 network common to all structures. The network topology of the Cu(tpt) network was confimed using the program SYSTRE.[18]

In the structure of {[Cu(tpt)(*o*-phthalate)]solvate}$_n$ the axes of Cu-tpt double helices are coincident with 3-fold screw axes as indicated in Figure 3(a) which shows that the helices are left-handed. If the bridging *o*-phthalate ligands are considered, the Cu centres of the two Cu-tpt helical strands are linked (Figure 3(a)). The resulting Cu-*o*-phthalate chain is a single helix with half the pitch of the Cu-tpt helix. The single Cu-*o*-phthalate helix has the opposite handedness to the Cu-tpt double helix i.e. right instead of left. A second type of crystallographic screw axis runs along relatively large channels in the crystal. The screw axes and the surrounding framework atoms are depicted in Figure 3b. Around this axis it is possible to identify Cu-tpt helices that are right-handed.

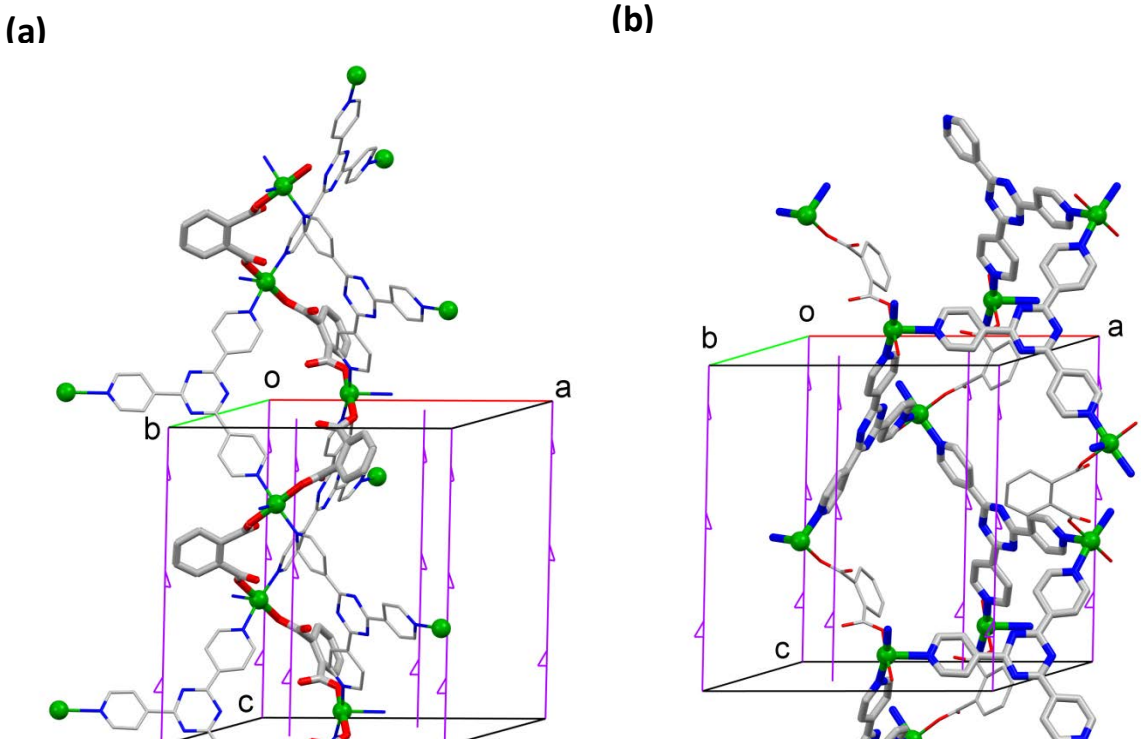

Figure 3. *Helical assemblies around the 3_1 axes at* ***(a)*** *$^1/_3$,$^2/_3$, z and* ***(b)*** *$^2/_3$, $^1/_3$, z in* {[Cu(tpt)(*o*-phthalate)]solvate}$_n$. *Cu centres are indicated by green spheres; o-phthalate ligands are indicated by thick connections in (a) and thin connections in (b), tpt ligands are indicated by thin connections in (a) and thick connections in (b).*

A characteristic of the 12,3 net is "self-entanglement" (or self-catenation) which relates to the fact that a connection of one 12-membered circuit passes through another 12-membered circuit within the same network. Certainly it is possible to identify examples of self-catenation in other single 3D networks, but a special feature of the 12,3 net is that the 12-membered circuit is the shortest circuit in the structure. Robson suggested that the self-catenation found in the 12,3 net is a consequence of the large number of nodes in a single circuit (12) resulting in the structure "folding back on itself". As with Robson's original network, catention of M_6tpt_6 rings is apparent, as is indicated in Figure 4(a). The bridging *o*-phthalate ligands serve as a brace between the catenated rings as is shown Figure 4(b).

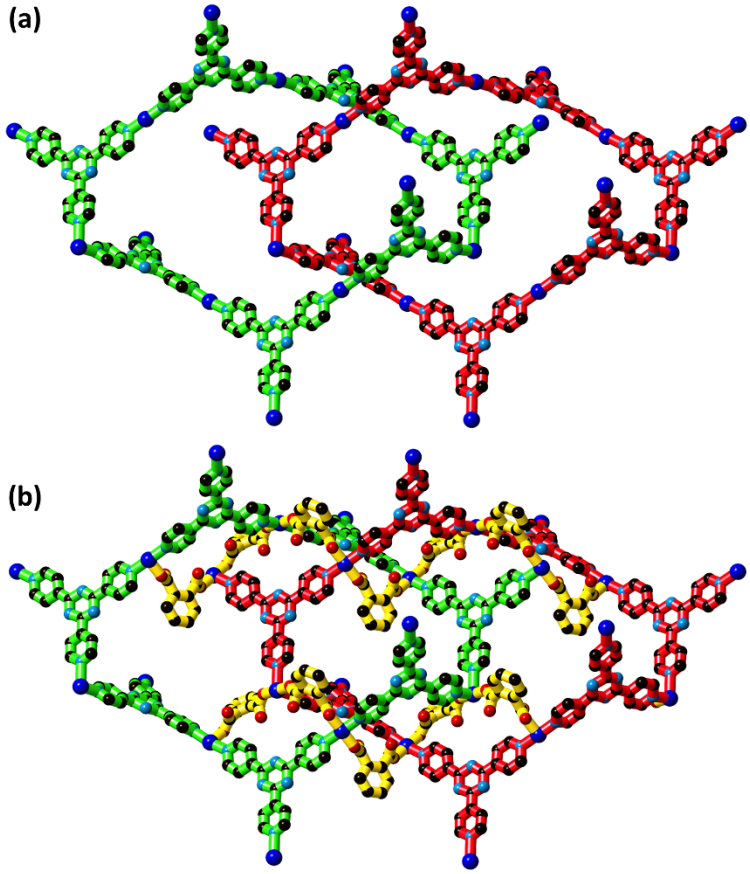

Figure 4. *Representations of a pair of Cu_6tpt_6 circuits (one with red bonds the other with green bonds) in $\{[Cu(tpt)(o\text{-phthalate})]solvate\}_n$ that form a catenane within the structure of $\{[Cu(tpt)(o\text{-phthalate})]solvate\}_n$ (a) without o-phthalate ligands and (b) with bridging o-phthalate ligands (indicated with yellow bonds).*

The relatively large channels parallel to the *c* axis (Figure 5(a)) are filled with disordered TCE molecules. These larger channels are connected by narrower channels parallel to the *a* and *b* axes (Figure 5(b)). SQUEEZE (probe radius 1.2 Å) gave the solvent accessible volume in the crystal as 2600 Å per cell, in other words 64.6% of the unit cell volume, and recovered 829 electrons. If all the disordered solvent is TCE, then this would correspond to 10 molecules of $C_2H_2Cl_4$ solvent per unit cell, or $3^1/_3$ molecules per formula unit (equivalent to 50.9 % of the mass) and giving an overall empirical formula of [Cu(tpt)(*o*-phthalate)]·$3^1/_3(C_2H_2Cl_4)$. The vacant axial coordination site is not directed into the main cavity.

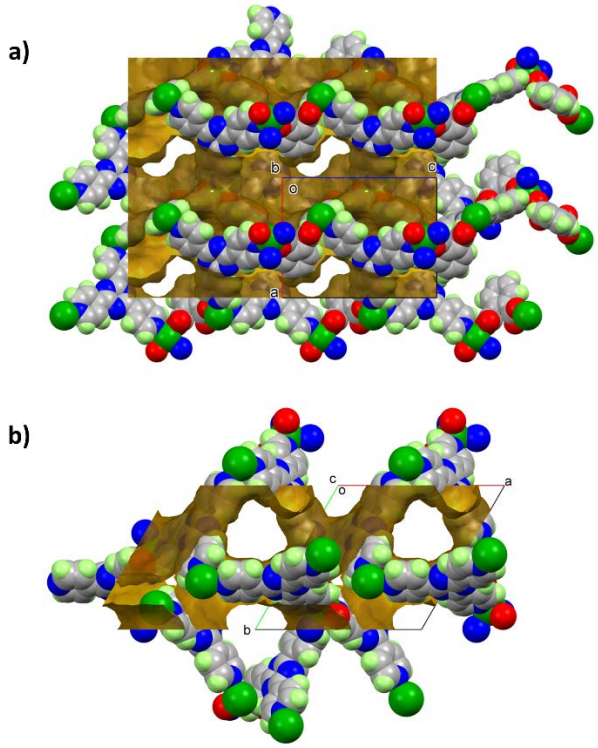

Figure 5. *Space filling representations of the large channels in {[Cu(tpt)(o-phthalate)]solvate}$_n$ viewed* ***a)*** *along the direction of the c axis (contact surface, radius 1.2Å[27,28]) and* ***b)*** *perpendicular to the direction of c-axis; narrow channels running parallel to the b axis are apparent.*

TGA measurements (Figure S1) on the bulk samples of {[Cu(tpt)(*o*-phthalate)]·$3^1/_3(C_2H_2Cl_4)$}$_n$ show a gradual mass loss of approximately 45 % as the temperature increases from 100 °C to 160 °C. Consistently, the boiling point of TCE is 147 °C. A mass loss of 45 % accords with approximately three molecules of TCE per formula unit in good agreement with the crystallographic data. The desolvated material is formulated as [Cu(tpt)(*o*-phthalate)]$_n$. Washing {[Cu(tpt)(*o*-phthalate)]·$3^1/_3(C_2H_2Cl_4)$}$_n$ with acetone also removes the TCE to give [Cu(tpt)(*o*-phthalate)]$_n$. With either method, a colour change from turquoise to pale blue-green occurs (Figure 6a).

Quantification of the Cu(II) content was achieved using EPR spectroscopy (Figure S2) concurring that {[Cu(tpt)(*o*-phthalate)]·$3^1/_3(C_2H_2Cl_4)$}$_n$ contains 6.3% (+/- 0.6). This furnishes more support for approximately three $C_2H_2Cl_4$ molecules per Cu site (theoretical 5.8 %). X-band EPR spectroscopy of powdered and crushed bulk samples of {[Cu(tpt)(*o*-phthalate)]·$3^1/_3(C_2H_2Cl_4)$}$_n$ and ground samples of single crystals of {[Cu(tpt)(*o*-phthalate)]·$3^1/_3(C_2H_2Cl_4)$}$_n$ exhibit similar EPR signals (Figure S3) with unresolved *g*-anisotropy and hyperfine structure due to the interaction of the unpaired electron on copper with the

nuclear spin of ^{63}Cu and ^{65}Cu (I = 3/2 for both isotopes). The partially unresolved features change somewhat depending on the content of TCE, the value of g_{av} = 2.14-2.13 is, however, almost constant.

Reversible Gas-Solid Reaction with Ammonia

When [Cu(tpt)(*o*-phthalate)]$_n$ (prepared by washing TCE out with acetone) is exposed to the ammonia vapour evolved from aqueous ammonia, it changes colour from pale blue-green to mauve within seconds (Figure 6(a) and (b)). Comparison of the IR spectra of [Cu(tpt)(*o*-phthalate)]$_n$ before and after exposure to ammonia reveals an N-H stretching band at 3343 cm^{-1} (Figure 7 red and purple) confirming the capture of ammonia. It is noteworthy that the uptake occurs under humid conditions and the material is stable at room temperature. The possibility that the guest is wholly or partially water can be rejected due to the absence of O-H bands. In addition, no color change is observed in the absence of ammonia. As discussed in detail later the uptake of ammonia is associated with a change of the EPR signal. The ammonia can be removed by heating to 200 °C to recover a green solid (Figure 6(c)). The N-H stretch in the IR spectrum concurrently disappears (Figure 7, green). The IR spectra of the solid before [Cu(tpt)(*o*-phthalate)]$_n$ is exposed to vapour from NH_3(aq) and after the removal of NH_3(aq) are identical (Figure 5 red and green).

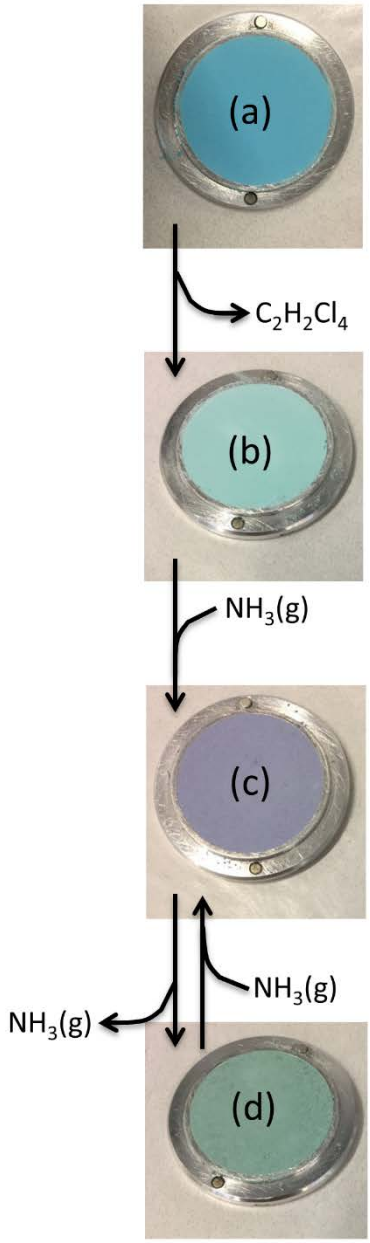

Figure 6. *Samples of [Cu(tpt)(o-phthalate)] indicating colour changes upon adsorption and desorption of solvate molecules and ammonia. (a) $\{[Cu(tpt)(o\text{-}phthalate)].3^1/_3(C_2H_2Cl_4)_3\}_n$. (b) Desolvated $[Cu(tpt)(o\text{-}phthalate)]_n$ produced by washing $\{[Cu(tpt)(o\text{-}phthalate)].3^1/_3(C_2H_2Cl_4)_3\}_n$ with acetone (c) $\{[Cu(tpt)(o\text{-}phthalate)(NH_3)_2]_n$ (d) $[Cu(tpt)(o\text{-}phthalate)]_n$ produced by heating $[Cu(tpt)(o\text{-}phthalate)(NH_3)_2]_n$ to 200 °C. The last step is reversible upon exposure to $NH_3(g)$.*

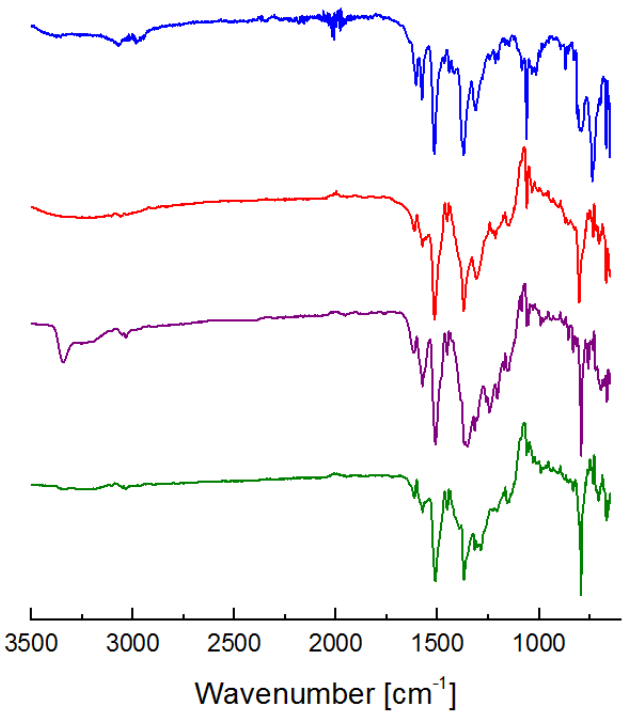

Figure 7. *FTIR spectra (ATR mode) of {[Cu(tpt)(o-phthalate)]3^1/$_3$($C_2H_2Cl_4$)$_3$}$_n$ (blue), [Cu(tpt)(o-phthalate)]$_n$ (red), [Cu(tpt)(o-phthalate)(NH_3)$_2$]$_n$ (purple) and {[Cu(tpt)(o-phthalate)]$_n$ (green) after removal of ammonia.*

TGA measurements verify a mass loss from the mauve material of 6.3 % when it is heated to 200 °C (Figure 8). This corresponds to two molecules of ammonia per Cu centre. Thus the ammonia adduct is formulated as [Cu(tpt)(*o*-phthalate)(NH_3)$_2$]$_n$. The de- and resorption of two ammonia molecules per Cu is reversible over ten cycles tried (Figure 8), without diminishing performance. There is no reason to expect that the sample would not be able to reversibly bind ammonia over many more cycles. After each removal, NH_3 reloading for 15 mins was performed outside of the TGA instrument. Increasing the loading time to 14 h did not increase the amount of ammonia taken up by the material. Mass loss begins around 150 °C suggesting that the ammonia interacts very strongly with the structure. This implies a chemisorptive mechanism (covalent bond formation with the host lattice) or very strong H-bonding.

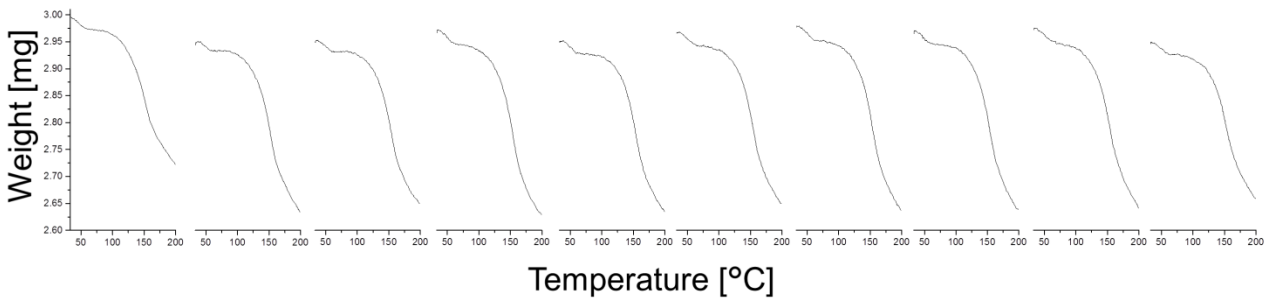

Figure 8. *TGA traces on ten repeat runs on one sample each indicating the release of ammonia from* $[Cu(tpt)(o\text{-phthalate})(NH_3)_2]_n$*. The resultant* $[Cu(tpt)(o\text{-phthalate})]_n$ *was reloaded ex-situ by exposure to vapour from aqueous ammonia over 15 mins.*

EPR spectroscopy was used to follow the absorption and desorption of ammonia in two different experimental setups. First a fractioned sample (>150 μm) of $\{[Cu(tpt)(o\text{-phthalate})]\cdot 3^1/_3(C_2H_2Cl_4)\}_n$ was exposed to a flow of dry He at room temperature *in situ* and subsequently exposed to a flow of dry 1 % NH_3 in He while monitoring with EPR spectroscopy (Figure 9). The initial signal displays a dominant contribution from Cu(II) with an average *g*-value of 2.14. During the flow of dry He the low field feature at 3000 Gauss is lost. After exposure to NH_3 the signal shifts to higher fields corresponding to a *g*-value of 2.12. The lower value suggests strongly that the Cu(II) is located in a 4N tetragonal plane perpendicular to the elongation axis. The fine structure of the signal is lost giving an almost completely isotropic EPR signal. In order to expel the NH_3 sorbed *in situ* the sample was then heated to 100 °C under a flow of He then cooled back to room temperature before obtaining a final spectrum. After this process the EPR signal is still featureless and isotropic and a little broader. The *g*-value returns to 2.14. The colours of the samples during this *in situ* treatment concur with those in Figure 6 during exposure to aqueous ammonia. The intensity of the EPR signal was determined as the double integral of the background corrected spectra and showed deviations (+/- 10 %) for the spectra shown.

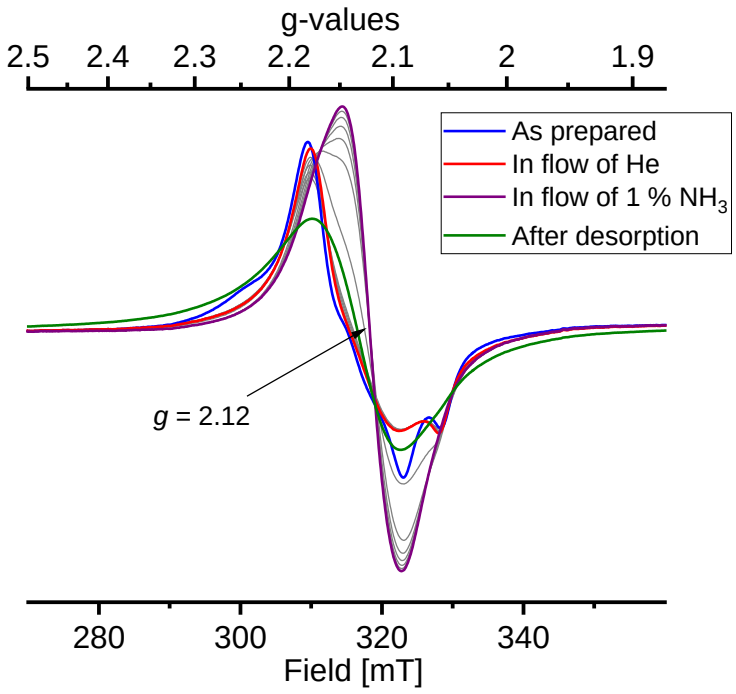

Figure 9. *In situ sorption and desorption of NH_3 followed by EPR spectroscopy. Blue: Starting spectrum from sample with homogenous particle size (predominantly $[Cu(tpt)(o\text{-phthalate})]_n$). Red during flow of He. Purple: With flow of 1% dry NH_3 (in He). Green: After desorption of guest NH_3.*

Secondly, an *ex-situ* experiment was devised to follow more closely the procedures used for the IR and TGA investigation. Desolvated $\{[Cu(tpt)(o\text{-phthalate})]\}_n$ (3.5 mg) was placed in a 4 mm EPR tube and measured (green trace in Figure S3). The tube was then placed in a closed container with 14 M NH_3 and left to absorb the atmosphere for an hour. The atmosphere in the narrow tube was stirred with a pipette a few times. NH_3 sorption was indicated by the colour change to mauve. The EPR spectrum was recorded and the tube was then heated to 150 °C and further to 175 °C with a few spectra obtained along the way. Finally, the sample in the tube was allowed to sorb NH_3 from the vapours above 14 M NH_3 once more. The series of EPR spectra are shown in Figure 10. The difference compared to the spectra that were produced by a flow of 1% NH_3 in He (Figure 9) are striking. Now clearly resolved individual EPR signals are seen for three different species. The spectrum of desolvated $[Cu(tpt)(o\text{-phthalate})]_n$ is clearly defined and shows an axial spectrum with resolved *g*-values at 2.075, 2.075 and 2.245 (green trace in Figure 10). The average *g*-value is 2.132. The completely NH_3 saturated sample, $[Cu(tpt)(o\text{-phthalate})(NH_3)_2]_n$ gives a rhombic spectrum with *g*-values at 2.053, 2.107, 2.155, with an average value 2.105 (dominant in the purple trace). Spectacularly, a third species is revealed on the way between these extremes with g-values 2.05, 2.10, 2.183. Average value 2.111. We suggest that this is intermediate $[[Cu(tpt)(o\text{-phthalate})(NH_3)]_n$ (dominant in the teal trace). Several isobestic points are present. The final spectrum (red-violet in Figure 10) shows the return to $[Cu(tpt)(o\text{-phthalate})(NH_3)_2]_n$. The intensity of the EPR spectra increased 13 % on the first absorption of ammonia and is constant within 4 % with subsequent treatments (Figure S4). The absorption of ammonia does not quite reach 100 % (2 NH_3 per Cu) in this particular experiment using a narrow tube, since a minor contribution (less than 30%) of $[Cu(tpt)(o\text{-phthalate})(NH_3)]_n$ can be recognized in both the spectra obtained.

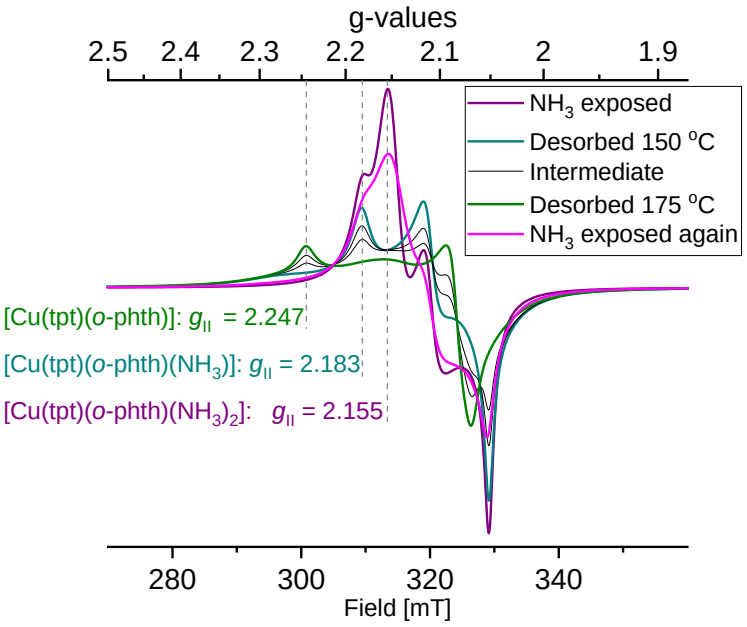

Figure 10. *Two-step sorption of NH_3 into [Cu(tpt)(o-phthalate)]$_n$ (green), with intermediate [Cu(tpt)(o-phthalate)(NH_3)]$_n$ (teal), and final product [Cu(tpt)(o-phthalate)(NH_3)$_2$]$_n$ (purple for the first and red-violet for the second cycle).*

Notably, no splitting due to hyperfine coupling to the copper nuclei as normally seen for Cu(II) compounds is evident in the EPR spectra of all three species. This suggests magnetic exchange between copper centres (Cu…Cu 7.8857(13) Å) contained within a well-defined crystal lattice. This has completely collapsed the normally observed splitting due to hyperfine coupling, but not the *g*-anisotropy. The line shape is predominantly Lorentzian. Exchange narrowing is described by Anderson[29] and has been observed to different extents for many copper systems, e.g., in a copper-amino complex by Calvo *et al*[30]. The elucidation of the magnetic coupling pattern in this system would be very interesting, but this has not yet been attempted.

The numerically highest *g*-value (g_{II} for axial systems) changes significantly during NH_3 sorption, decreasing by 0.06 with the first NH_3 entering the structure and additionally by 0.03 with the second (Figure 10). The trend in the average *g*-values are the same as was observed during the *in situ* measurements (Figure S3). The trend and the values are in complete accord with strong nitrogen donors taking the place of oxygen in the plane perpendicular to the elongation axis around a typical tetragonal Cu(II) center.

In conclusion, the impressive EPR spectra shown in Figure 10 are the result of exchange coupling between crystallographically equivalent but magnetically distinct Cu centers in combination with high crystallinity. The three Cu centers of the unit cell are locked in magnetic exchange that result in a particular and unusual

coupling pattern. Small pertubations away from the strict symmetry destroy the anisotropic features of the EPR spectrum resulting in spectra showing complete collapse of the fine-structure. The fresh samples with some absorbed water, and the *in situ* sample (which had first been fractioned and then exposed to gas flows, Figure 9) experience too many deviations in the magnetic coupling pattern resulting in a more randomized collapse of the fine structure. By contrast, the pristine, carefully absorbed and gently desorbed sample retains the *g*-anisotropy and loses the hyperfine structure completely. Some percentage of the EPR signal intensity of the green spectrum in Figure 10 (the small bump in the middle) has the completely collapsed structure, and the features of the pink trace are less sharp compared to the purple trace, so a detectable amount of additional defects have appeared in the sample after one desorption procedure. The PXRD patterns for $[Cu(tpt)(o\text{-phthalate})]_n$ and $[Cu(tpt)(o\text{-phthalate})(NH_3)_2]_n$ (Figure S5) show significant crystallinity, however, with some broadening suggesting that some of the long range order structure is lost during the desorption of TCE and the absorption of ammonia as was implied by the EPR spectroscopy on identically treated samples. The diffraction patterns show changes consistent with crystal phase transitions during each of the desorption and sorption processes.

The colour changes, apparent stoichiometry of two NH_3 per Cu site, crystal phase changes and appropriate shifts of the *g*-values to indicate 4N equatorial coordination for the NH_3 loaded phase, all point strongly to a highly selective chemisorption process for NH_3 into $[Cu(tpt)(o\text{-phthalate})]_n$. While we can only speculate, we believe that the observations made so far entitle us this liberty. We suggest that precisely two guest NH_3 molecules can coordinate to the Cu(II) sites and that this is enabled by the de-coordination of an equatorial *o*-phthalato donor. Coulombic forces must be overcome for this to happen, so this might seem surprising. However, de-coordination will be assisted if this ligand is in an axial position of the Jahn-Teller distorted ion. H-bonding to an inserted ammonia will also compensate. Of some relevance perhaps is the minor disorder of this group in the crystal structure which might indicate flexibility. This would then be involved in H-bonding to the coordinated amine that has replaced it, hence the highly distinguishable $\nu_{N\text{-}H}$ in the IR spectrum. The other amine ligand could then occupy the formally vacant axial site, Figure 11. We recognise that this site was not pointing towards the solvent accessible void space in the starting structure of $\{[Cu(tpt)(o\text{-phthalate})].3^1/_3(C_2H_2Cl_4)_3\}_n$. However, with the removal of so much co-crystallised TCE from the exceptionally large solvent accessible voids (65%), a significant structural distortion can be expected. As a consequence, this vacant axial copper binding site becomes accessible to the void space. The binding of a ammonia may then trigger a “loosening" of the equatorial *o*-phthalato donor to allows for insertion and coordination of the second NH_3. This speculation is in accordance with the EPR results that show stronger donating ligands in the equatorial plane. Note that the elongation axis in the tetragonal

coordination around copper could easily change from N_2O_2 to N_2N_2 at the active copper(II) site. A depiction of this proposed mechanism is presented in Figure 12.

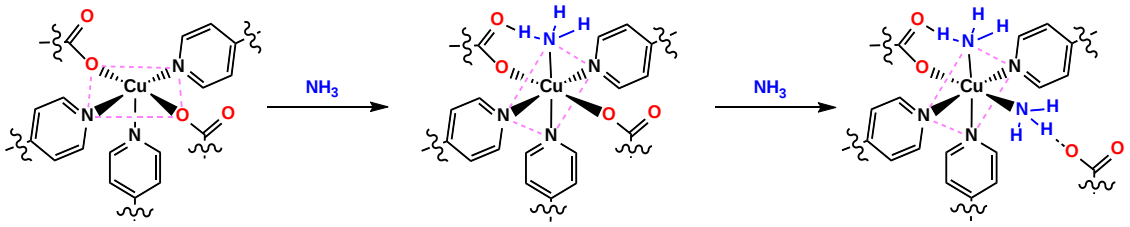

Figure 11. *Structural proposal for the stepwise reversible chemisorption of two ammonia molecules per active Cu(II) site in* $[Cu(tpt)(o\text{-phthalate})]_n$. *The basal equatorial plane is indicated by the pink dashed lines.*

Conclusion

In this investigation of copper 2,4,6-tri-4-pyridyl-1,3,5-triazine networks the synthesis and structural characterisation of a new porous Cu(II) coordination polymer has been achieved. The Cu-tpt network adopts the unusual 12,3 topology with the Cu(II) centres serving as T-connectors and the tpt ligands acting as regular trigonal connectors. Within the 3D network *o*-phthalate ligands act as additional bridges between Cu(II) centres. The structure is closely related to that of [Ni(tpt)$(NO_3)_2$·solvate] and [Ni(tpt)(o-phthalate)$_2H_2O$·solvate] which share the same metal-tpt topology. Crystals of [Ni(tpt)$(NO_3)_2$·solvate] were shown to be relatively sensitive to solvent loss whilst [Ni(tpt)(o-phthalate)$_2H_2O$·solvate] was able to undergo desolvation and act as a gas adsorbent. Presumably the *o*-phathalate ligand's ability to act as a "brace", in linking helical M-tpt strands, results in the generation of a more robust network material. Bridging *o*-phthalate ligands also appear to provide structural support to the Cu-tpt network, allowing the compound to also act as a host coordination polymer. The incorporation of Cu(II) in place of Ni(II) offers the prospect of guests binding directly to the metal centre. Remarkably, the adsorption of the ammonia is unaffected by water vapour with no adsorption of water even under high humidity ammonia streams. Furthermore the sample exhibits no loss of performance with respect to its porosity through continuous cycles of adsorption and desorption.

Spectroscopic techniques along with thermogravimetric analysis have proved to be informative in following the adsorption and desorption of ammonia. EPR spectroscopy in particular has been shown to be a powerful tool for elucidating changes in the environment of the Cu(II) centre associated with the coordination of ammonia. Clearly, there is great scope for using EPR to probe changes in coordination environments of paramagnetic metal ions when they are incorporated into porous network materials.

The presence of vacant coordination sites within the [Cu(tpt)(*o*-phthalate)] network offers the prospect of introducing ligands that become tethered to the framework but have functional groups extending into the channels. Given the demonstrated porosity of this system it may be possible to introduce reagents that are able to combine with appropriately functionalised ligands within the chiral channels. Under these circumstances any reaction that might be promoted within this asymmetric, geometrically confined space may be different to those that would be generated in the absence of the host framework.

Supporting Information

TGA of $\{[Cu(tpt)(o\text{-phthalate})]\cdot 3^1/_3(C_2H_2Cl_4)\}_n$. EPR spectra of powdered bulk samples and powdered single crystals of $\{[Cu(tpt)(o\text{-phthalate})](C_2H_2Cl_4)_3\}_n$, $[Cu(tpt)(o\text{-phthalate})]_n$ and $[Cu(tpt)(o\text{-phthalate})_n(NH_3)_{2n}]$ produced in situ by a flow of NH_3 in He. CCDC 1905857 for the structure of $\{[Cu(tpt)(o\text{-phthalate})]\cdot 3^1/_3(C_2H_2Cl_4)\}_n$.

AUTHOR INFORMATION

Corresponding Author

E-mail: mckenzie@sdu.dk. Phone: +45 6550 2518

ORCID

Christina Wegeberg 0000-0002-6034-453X

David Nielsen 0000-0002-7764-1151

Susanne Mossin 0000-0001-7763-9660

Brendan F. Abrahams 0000-0003-2957-860X

Vickie McKee 0000-0002-7780-5814

Christine J. McKenzie 0000-0001-5587-0626

Notes

The authors declare no competing financial interest

This research did not receive any specific funding.

References

[1] H. Furukawa, K. E. Cordova, M. O'Keeffe, O. M. Yaghi, *Science* **2013**, *341*, 1230444.

[2] S. Kitagawa, R. Kitaura, S. Noro, Angew. Chem. Int. Ed. Engl. ***2004****, 43, 2334–2375.*

[3] J.-R. Li, R. J. Kuppler, H.-C. Zhou, Chem. Soc. Rev. ***2009****, 38, 1477–1504.*

[4] X. Fang, B. Zong, S. Mao, Nano-Micro Lett. ***2018****, 10, 64.*

[5] H. Wang, W. P. Lustig, J. Li, Chem. Soc. Rev. ***2018****, 47, 4729–4756.*

[6] X. Zhao, Y. Wang, D.-S. Li, X. Bu, P. Feng, Adv. Mater. Weinheim ***2018****, 30, e1705189.*

[7] J. Zhang, Z. Chen, J. Chromatogr. A ***2017****, 1530, 1–18.*

[8] B. Timmer, W. Olthuis, A. van den Berg, Sensors and Actuators B: Chemical ***2005****, 107, 666–677.*

[9] G. W. Peterson, G. W. Wagner, A. Balboa, J. Mahle, T. Sewell, C. J. Karwacki, J. Phys. Chem. C, Nanomater. Interfaces ***2009****, 113, 13906–13917.*

[10] T. Kajiwara, M. Higuchi, D. Watanabe, H. Higashimura, T. Yamada, H. Kitagawa, Chem. Eur. J ***2014****, 20, 15611–15617.*

[11] M. G. Campbell, D. Sheberla, S. F. Liu, T. M. Swager, M. Dincă, Angew. Chem. Int. Ed. Engl. ***2015****, 54, 4349–4352.*

[12] A. Godiksen, F. N. Stappen, P. N. R. Vennestrøm, F. Giordanino, S. B. Rasmussen, L. F. Lundegaard, S. Mossin, J. Phys. Chem. C ***2014****, 118, 23126–23138.*

[13] H. L. Anderson, S. Anderson, J. K. M. Sanders, J. Chem. Soc., Perkin Trans. 1 ***1995****, 2231.*

[14] G. M. Sheldrick, SADABS V2012/1, University Of Göttingen, Germany, ***1996****.*

[15] G. M. Sheldrick, Acta Crystallogr. A Found. Adv. ***2015****, 71, 3–8.*

[16] G. M. Sheldrick, Acta Crystallogr. C Struct. Chem. ***2015****, 71, 3–8.*

[17] A. L. Spek, Acta Crystallogr. C Struct. Chem. ***2015****, 71, 9–18.*

*[18] Systre - Program for the analysis of periodic nets v 19.6.0 O. Delgado-Friedrichs **2019**, gavrog.org*

*[19] A. F. Wells, Three-Dimensional Nets and Polyhedra, Wiley, New York, **1977**.*

*[20] A. F. Wells, Further Studies Of Three-dimensional Nets (aca Monograph, No 8), Amer Crystallographic Assn, New York], **1979**.*

[21] M. O'Keeffe, M. A. Peskov, S. J. Ramsden, O. M. Yaghi, O. M. *Accts. Chem. Res.* **2008**, *41*, 1782-1789

*[22] B. F. Hoskins, R. Robson, J. Am. Chem. Soc. **1990**, 112, 1546–1554.*

*[23] R. Robson, B. F. Abrahams, S. R. Batten, R. W. Gable, B. F. Hoskins, J. Liu, in Supramolecular Architecture: Synthetic Control in Thin Films and Solids (Ed.: T. Bein), American Chemical Society, Washington, DC, **1992**, pp. 256–273.*

[24] M. O'Keeffe, B. G. Hyde, *Crystal Structures I: Patterns and Symmetry*. *Min Soc. Amer., Washington D.C.*, *USA*, **1996**.

*[25] B. F. Abrahams, S. R. Batten, M. J. Grannas, H. Hamit, B. F. Hoskins, R. Robson, Angew. Chem. Int. Ed. **1999**, 38, 1475–1477.*

*[26] D.-S. Zhang, Z. Chang, Y.-F. Li, Z.-Y. Jiang, Z.-H. Xuan, Y.-H. Zhang, J.-R. Li, Q. Chen, T.-L. Hu, X.-H. Bu, Sci. Rep. **2013**, 3, 3312.*

*[27] C. F. Macrae, P. R. Edgington, P. McCabe, E. Pidcock, G. P. Shields, R. Taylor, M. Towler, J. van de Streek, J Appl Crystallogr **2006**, 39, 453–457.*

*[28] C. F. Macrae, I. J. Bruno, J. A. Chisholm, P. R. Edgington, P. McCabe, E. Pidcock, L. Rodriguez-Monge, R. Taylor, J. van de Streek, P. A. Wood, J Appl Crystallogr **2008**, 41, 466–470.*

*[29] P. W. Anderson, P. R. Weiss, Rev. Mod. Phys. **1953**, 25, 269–276.*

*[30] R. Calvo, H. Isern, M. A. Mesa, Chem Phys **1985**, 100, 89–99.*

TOC

Reversible and Vapochromic Chemisorption of Ammonia by a Copper(II) Coordination Polymer

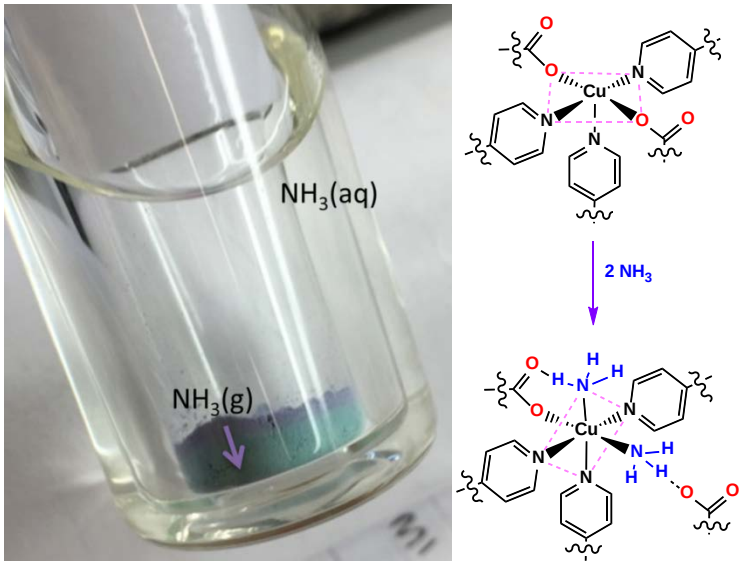

The coordination polymer {[Cu(tpt)(*o*-phthalate)]·$3^{1}/_{3}$(TCE)}$_n$ (tpt = 2,4,6-tri-4-pyridyl-1,3,5-triazine, TCE = 1,1,2,2-tetrachloroethane) has a 12,3 net. Removal of TCE produces a pale green crystalline phase which chemisorbs two equivalents of ammonia per Cu site. The mauve ammonia adduct is stable up to ca. 150 °C before the reversible desorption of the chemisorbed guest (minimum 10 cycles). EPR spectroscopy shows changes in *g*-values suggestive of two-step chemisorption with Cu-amine bonding in the loaded phase.